Design and Analysis of a Ferrite-PM-Assisted Hybrid Reluctance Machine for Electric Vehicle Propulsion

Weiyu Wang
Department of Electrical Engineering
The Hong Kong Polytechnic University
Hong Kong, China
weiyu.wang@connect.polyu.hk

Xing Zhao
Department of Electrical Engineering
The Hong Kong Polytechnic University
Hong Kong, China
xing.zhao@polyu.edu.hk

Sigao Wang
Department of Electrical Engineering
The Hong Kong Polytechnic University
Hong Kong, China
18106301r@connect.polyu.hk

Shuangxia Niu
Department of Electrical Engineering
The Hong Kong Polytechnic University
Hong Kong, China
eesxniu@polyu.edu.hk

Qingsong Wang
Département de génie électrique
École de technologie supérieure
Montreal, Canada
Qingsong.Wang@etsmtl.ca

IECON 2021 - 47th Annual Conference of the IEEE Industrial Electronics Society | 978-1-6654-3554-3/21/$31.00 ©2021 IEEE | DOI: 10.1109/IECON48115.2021.9589781

***Abstract*— Reluctance machines with DC field coil in the stator is a competitive candidate for electric vehicle propulsion due to the elimination of rare-earth permanent magnets (PM), robust structures and controllable excitation. However, their torque density cannot be compared with PM machines. Introducing rare-earth PMs into reluctance machines can be an effective way to boost torque density, but the costs will greatly increase as well. To solve this problem, this paper proposes a hybrid reluctance motor using assistive ferrite magnets in stator slots. The introduced ferrite magnets operate based on the flux modulation effect for torque density improvement. It is revealed by finite element analysis, with ferrite magnets in stator slots, machine torque density and efficiency can be improved by 20.2% and 5.1%, respectively.**

***Keywords*— hybrid reluctance machine, ferrite magnets, flux modulation, torque density**

I. Introduction

Due to high torque density and high efficiency, the rare-earth permanent magnet (PM) machines have been widely applied in electrical vehicles and more electric aircraft propulsion systems [1-6]. However, the rare-earth PM material is a non-renewable resource, and its price is oscillating with supply status. Therefore, the non-PM reluctance machines have attracted wide attention in the literature [1]. As a typical non-PM machine, switched reluctance machine (SRM) has the advantages of a simple structure, high reliability, and low cost. However, each phase of SRM is only energized in the first quadrant of the BH curve to provide pulse torque generation, thus the torque ripple is large, while the torque density is poor [7]. To improve torque density, auxiliary rare-earth PMs can be introduced into stator slots to extend its BH working range [12].

Doubly-fed doubly salient motor (DF-DSM) has a similar rotor and stator structure with SRM but with additional DC field coils in the stator. Alternating excitation flux can be established by DC field coils, which enables DF-DSM to operate in a whole electrical period [13]. However, its torque density is lower than that of SRM since the space of the stator slot is shared by DC coils and AC coils. The torque ripple is still serious because of the rich even-order harmonics and the unbalanced magnetic circuit between phases. Variable flux reluctance machine (VFRM), as an improved topology, can be designed with more flexible slot pole combinations. Especially for the odd rotor pole design, the rich even-order flux harmonics can be eliminated, meanwhile, the symmetrical voltage and constant inductance are acquired. Therefore, the torque ripple and cogging torque are reduced [16], while the torque density is still lower than that of SRMs.

A hybrid reluctance machine (HRM) is proposed for electric vehicle propulsion [17-18], in which a small amount of rare-earth PMs are embedded in stator slots to generate flux modulation effect and interact with the redundant harmonics of armature winding. In this way, the torque density and efficiency can be significantly improved. In addition, the flux linkage of DC and PM excitation share a parallel magnetic circuit, which enables a bidirectional field regulation to extend the speed range. However, this machine still uses rare-earth PMs, which increases the cost and reduces machine reliability. As a nonrenewable resource, the rare-earth PMs should be replaced by accessible materials. The application of ferrite magnets in electrical machines is an effective way to remove rare-earth PMs [19], although its coercivity and remanence are lower than that of rare-earth PMs. As an artificial material, ferrite magnets have quite lower prices. In addition, ferrite magnets have less core loss and eddy current loss due to their low conductivity. Based on the tradeoff between production costs and torque density, a ferrite-assisted HRM for electric vehicle propulsion is proposed in this paper. In Section II, the machine structure and operation principle are introduced. In Section III, four models with different slot pole combinations are compared including magnetic field distribution, flux linkage, phase inductance, cogging torque and back electromotive force. Then, the effect of using ferrite magnets and NdFeB35 in terms of torque density is presented. In Section IV, the electromagnetic performance of the optimal design is analyzed. Finally, some conclusions are drawn in Section V.

II. THE PROPOSED HYBRID RELUCTANCE MACHINE

A. Machine configuration

The structure of the proposed ferrite-PM-assisted HRM is presented in Fig .1. It uses a doubly salient structure. On the stator side, two sets of winding are adopted, namely DC field winding and AC armature coils. The ferrite magnets are magnetized in the radial outward direction and mounted on the slot openings. On the rotor side, there is only an iron core, thus providing mechanical robustness**.** To further explain the flux modulation principle of the DC field winding and ferrite magnets, the magnetic circuit of two excitation sources is denoted in Fig. 1 as well. It is clear to see that the magnetic circuit of DC field winding is relatively short and cycled the wounded stator teeth, airgap and adjacent rotor teeth. The magnetic circuit of ferrite magnets is longer in the parts of the stator yoke and rotor yoke. However, the flux linkage generated by two excitation sources has the same electrical frequency and phase angle and thus can be overlapped effectively. In addition, the ferrite magnets are exposed to less demagnetization risk as no armature flux linkage passes them. In general, the proposed ferrite-PM-assisted HRM has a robust structure, low cost, improved torque density and efficiency at the same time, which can be an attractive solution for EVs.

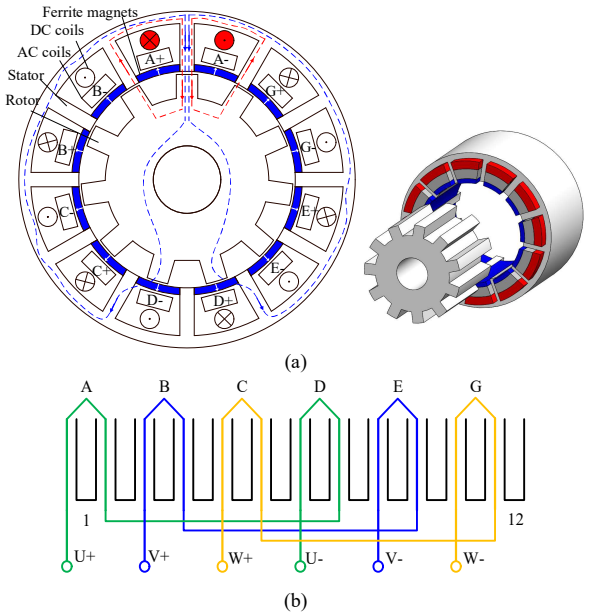

Fig. 1. (a) Structure of the proposed HRM. (b) AC winding connections.

B. Flux modulation effect of slot PMs

Based on the principle of flux modulation [20-22], the magnetic poles are formed by the ferrite magnets and the adjacent stator tooth. Furthermore, the ferrite magnet field is modulated by rotor salient poles. Meanwhile, abundant air gap harmonics are generated to boost torque generation. The rotational speed $v_{i,j}$ and the pole pair number $PPN_{i,j}$ can be illustrated as

$$\begin{cases} v_{i,j}=\dfrac{jn_r}{in_s+jn_r}\omega_r \\ PPN_{i,j}=|in_s \pm jn_r| \end{cases}, \quad i=1, 3, 5\ldots, j=0, 1, 2, 3\ldots \tag{1}$$

where n_s is the pole pair number of ferrite magnets, n_r is the pole pair number of rotor poles, ω_r is rotor mechanical angular velocity. The dominant components of air gap harmonicas after the modulation are further concluded in Table I.

TABLE I. DOMINANT HARMONICS EXCITED BY FERRITE MAGNETS

	i=1, j=0	i=1, j=1	
$v_{i,j}$	0	n_s+n_r	$\lvert n_s-n_r\rvert$
$PPN_{i,j}$	n_s	$\dfrac{n_r}{n_s+n_r}\omega_r$	$\dfrac{n_r}{n_s-n_r}\omega_r$

When i=1, j=0, the rotational speed is 0, thus there is no effective flux linkage and electromagnetic torque produced. When i=1, j=1, two main working harmonics generated by ferrite magnets are generated after rotor generation. and their rotating direction is opposite. And to transmit the maximum electromagnetic torque with ferrite magnets harmonics, the pole pair number of AC armature winding can be designed by

$$n_a=|n_s-n_r| \tag{2}$$

Further, the magnetic gearing ratio can be described as (3).

$$G_r=\frac{n_s}{n_a} \tag{3}$$

The electromagnetic torque produced by ferrite magnets can be further expressed as

$$T=\frac{3}{2}krln_r\frac{B_p}{G_r}NI \tag{4}$$

where k is the fundamental winding factor, r is the air-gap radius, l is the stack length, B_p is the amplitude of harmonic flux density, and NI is the winding ampere-turns.

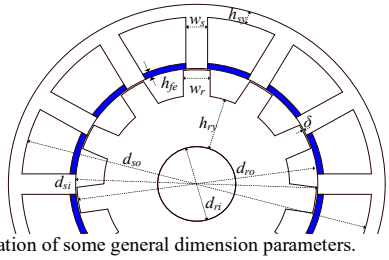

Fig. 2. Illustration of some general dimension parameters.

TABLE II. DESIGN PARAMETERS FOR THE PROPOSED MACHINE

Symbol	Parameter	Unit	Value
d_{so}	Outer diameter of stator	mm	130
d_{ri}	Inner diameter of stator	mm	90
d_{ro}	Outer diameter of rotor	mm	89
d_{si}	Inner diameter of rotor	mm	60
h_{ry}	Height of rotor yoke	mm	20
h_{sy}	Height of stator yoke	mm	5
h_{fe}	Height of ferrite magnets	mm	Variable
δ	Air gap length	mm	0.5
l	Stack length	mm	80
w_s	Width of stator teeth	mm	Variable
w_r	Width of rotor teeth	mm	Variable
	Turns of each DC coil		80
	Turns of each AC coil		80
	Slot factor		0.7
	Rated current density	A/mm^2	6
	Rated speed	rpm	2500

III. Design Considerations

A. Pole-pair Combinations

In this paper, four-slot pole combinations of proposed HRM are compared including the 12/10, 12/11, 12/13 and 12/14 cases. Fig .2 shows the general dimension parameters, and the detailed specifications are listed in Table II.

Fig .3 and Fig .4 show the no-load flux linkage distributions with different slot pole combinations. In addition, consistent with the above analysis, the DC excitation magnetic circuit mainly follows the wounded stator teeth, adjacent stator teeth and meshing rotor teeth. Due to the bipolarity of the ferrite magnets magnetic circuit and the phase consistency with the DC excitation magnetic circuit, the variation range of the composite magnetic circuit will be enhanced.

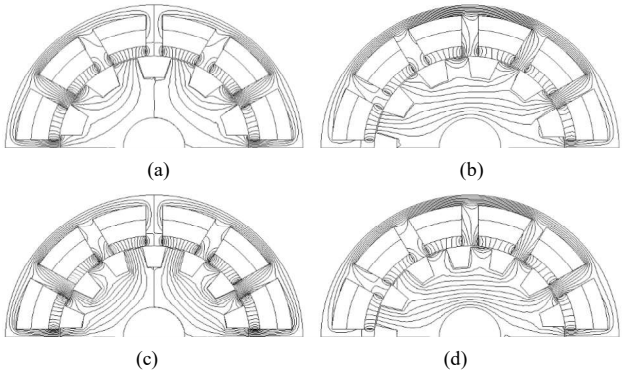

Fig .3. No-load magnetic field distribution generated by ferrite magnets only. (a) 12/10. (b) 12/11. (c) 12/13. (d) 12/14.

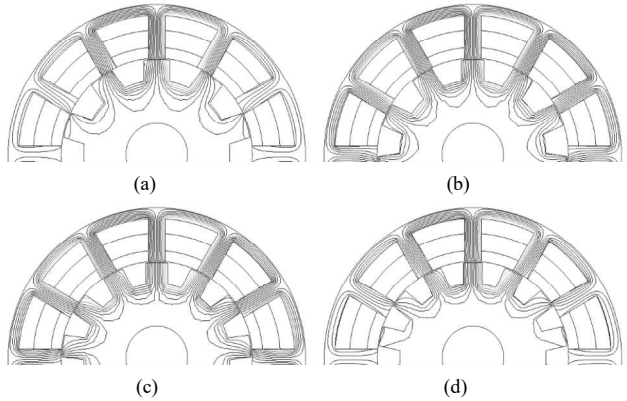

Fig .4. No-load magnetic field distribution generated by DC field source only. (a) 12/10. (b) 12/11. (c) 12/13. (d) 12/14.

Fig .5 shows the flux linkage and harmonics distribution of four models, under different excitation statuses. When only DC is active, as shown in Fig. 5(a), it is clear to see that the flux linkage of 12/11 and 12/13 are symmetrical, while that of 12/10 and 12/14 is offset. When only ferrite magnets are active, the flux linkage is always bipolar and symmetrical as shown in Fig .5(b), regardless of the slot pole combinations. In Fig .5(c), the sum of flux linkage produced by dual sources is presented. The synthetic flux linkage for 12/11 and 12/13 designs is still symmetrical, while that of 12/10 and 12/14 is biased. The magnitude of the flux linkage is increased, which means dual excitation sources can effectively work at the same time. Further, the harmonics distribution excited by dual sources is analyzed and presented in Fig .5(d). The even-order harmonics of 12/11 and 12/13 cases are eliminated due to the electromagnetic complementary characteristic. In addition, the 12/11 case performs the biggest fundamental component of flux linkage, which contributes to torque generation.

With different slot pole combinations, the self-inductance curves are quite distinctive as presented in Fig .6. Those of 12/10 and 12/14 vary significantly with the electrical angle, while the self-inductance curves of 12/11 and 12/13 show fewer fluctuations during the whole electrical period. Usually, smooth self-inductance can help to achieve a better current control effect when supplied by pulse-width-modulation inverters.

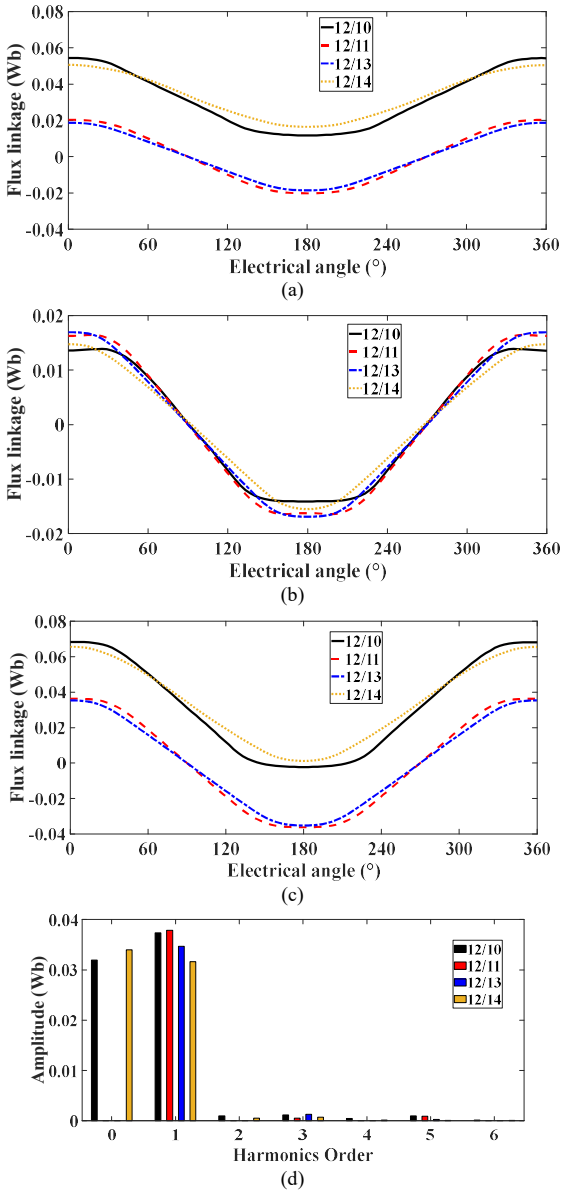

Fig .5. Phase flux linkage. (a) DC excited only. (b) Ferrite magnets excited only. (c) Dual sources excited. (d) Harmonics distributions of dual sources.

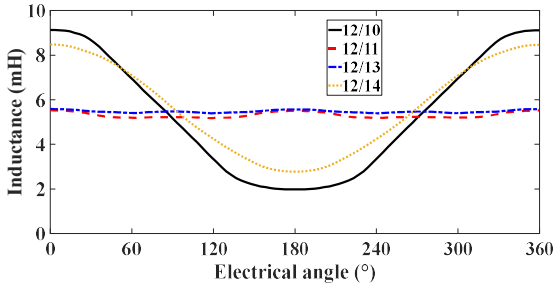

Fig .6. Self-inductance waveforms.

The cogging torque produces an extremely decisive impact on the vibration and noise of the machines. For salient pole machines, the matching of stator magnetic poles and rotor teeth has a crucial influence on torque ripple. The smaller the least common multiple of the number of magnetic poles and rotor teeth is, the greater the torque fluctuation occurs [23]. As shown in Fig .7, the cogging torques of 12/11 and 12/13 are quite smaller than those of 12/10 and 12/14. The induced voltages under a no-load situation are calculated and presented in Fig .8. Compared with 12/10 and 12/14 cases, the induced voltage of 12/11 and 12/13 cases are more symmetrical. Based on the above analysis, the 12/11 case synchronously obtains symmetrical flux linkage, back EMF, minimum cogging torque, and thus selected as the optimal design for further analysis.

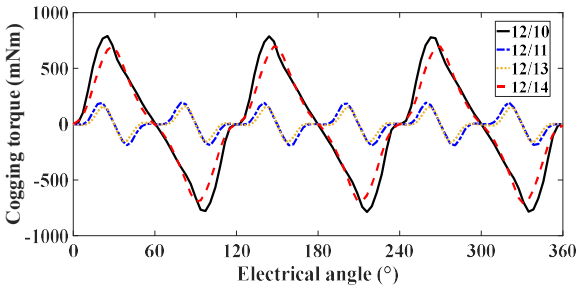

Fig .7. Cogging torque excited by dual sources

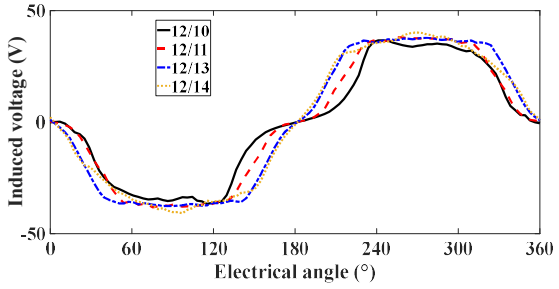

Fig .8. Induced voltage excited by dual sources

B. Comparative study of ferrite magnets and NdFeB35

The effect of two different PM materials on the performance of the proposed HRM are evaluated in this part, including the popular rare-earth PM of NdFeB35 and ferrite magnets, hence to determine the suitable amount of ferrite magnets applied in stator slots. The parameters and specifications of NdFeB35 and ferrite magnets are listed in Table III. Although the remanence and coercive of ferrite magnets are relatively lower, the price of them is only about 10% of NdFeB35.

The usages of ferrite magnets and NdFeB35 in the proposed machine are compared in Fig .9. For a fair comparison, all the design parameters keep the same except the height of PMs. For NdFeB35, the maximum average torque can be acquired by introducing 3mm height usage. While for ferrite magnets, the peak point of the average torque curve occurs at around 4mm usage. Although the torque improvement with ferrite magnets is less than that of NdFeB35, the cost is much lower. In addition, after reaching their peak points, both torque curves fall. This is part of magnetic saturation, meanwhile, the redundant magnetic material takes up the space of the windings, leads to a decrease of the electrical load and average torque. When the height of the magnet exceeds 7.7mm, the torque generated by the ferrite-assisted HRM is greater than that when using NdFeB35. The optimal usage of ferrite magnets is selected as 4mm height to acquire the maximum average torque. Through FEA, at 4mm height usage, the core loss produced by ferrite-assisted HRM is lower than that of NdFeB35-assisted HRM.

TABLE III. MAJOR MATERIALS AND SPECIFICATIONS

Material	Remanence	Coercive force	Price
Ferrite magnets	0.4 T	300 kA/m	40$/kg
NdFeB35	1.2 T	915 kA/m	4$/kg

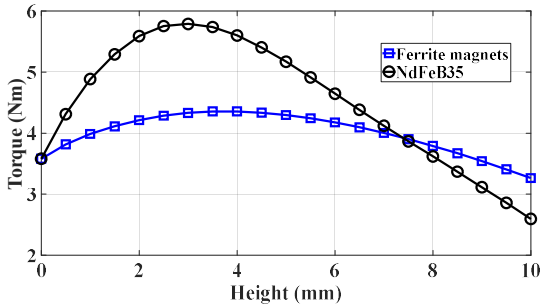

Fig .9. Average torque under different heights of ferrite magnets and NdFeB35.

IV. ELECTROMAGNETIC PERFORMANCE ANALYSIS

To further verify the flux modulation effect, DC excitation, ferrite magnets excitation and AC excitation are calculated by FEA, respectively. Based on the flux modulation principle, if these exciting harmonics and AC harmonics have the same rotational speed and the same pole pair number, the torque density can be improved. Fig .10 (a) shows the flux density with only DC field excitation and its fast Fourier transform (FFT). Fig .10(b) describes the flux density and its FFT of the main harmonic components excited by ferrite magnets only. The orders of these dominant harmonic components are quite different. Compared with the redundant harmonics excited by AC coils with a single-layer concentrated winding design, DC excitation and ferrite magnets excitation can work together and contributes to enhanced torque generation.

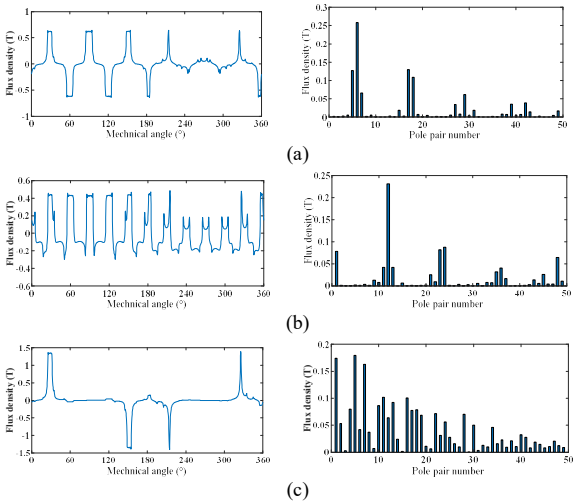

Fig. 10. Flux density in the air gap and its harmonics distribution. (a) Only DC 6A. (b) Only ferrite magnets. (c) Only AC armature current 6A.

The flux density distributions at different excitation statuses are shown in Fig .11. With DC field excitation, the flux density is relatively low, which means there is room for improving core utilization. With extra ferrite magnets active, the magnetic field density is increased but does not show severe saturation, and no risk of demagnetization. Fig. 12 shows the torque curves of the proposed ferrite-assisted HRM at different excitation statuses. It is shown that 20.2% torque improvement can be achieved by ferrite assistance. The comparison of efficiency can be found in Fig .13. Compared with DC excitation only, the efficiency of ferrite-assisted HRM can be improved by 5.1% at the rated speed.

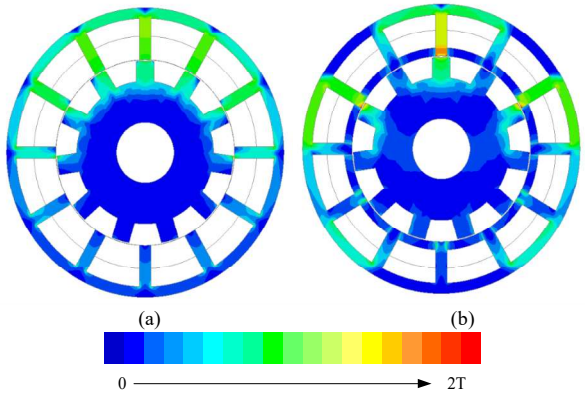

Fig .11. Magnetic field density. (a) DC excited only. (b) DC and ferrite magnets.

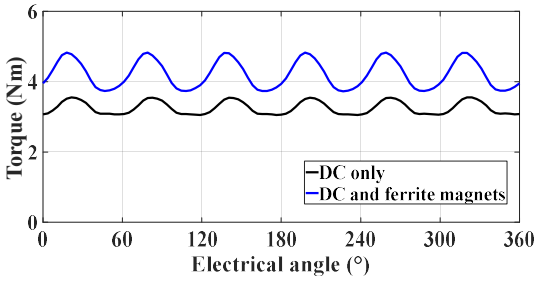

Fig .12. Steady torque curves at different excitation status

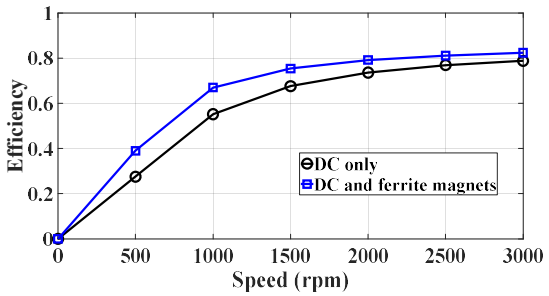

Fig .13. Calculated efficiency at different speeds.

V. Conclusion

This paper proposes a novel ferrite-assisted HRM for electric vehicle propulsion. The key is to evoke flux modulation effect by introducing ferrite magnets into stator slots. By using FEA, the effect of torque density improvement has been testified. The torque density and the efficiency can be improved by 20.2% and 5.1%, respectively. The 12/11 structure is a proper slot pole combination. The comparisons between rare-earth PMs and ferrite design are compared in terms of torque density and cost. In conclusion, using ferrite assistance can be seen as a strategy to improve torque density performance and save costs at the same time. Hence, the proposed ferrite-assisted HRM presents the potential to be widely used in the electric vehicle industry.

Acknowledgment

This work was supported by Project No. PolyU 152509/16E from the Hong Kong Research Grants Council, Hong Kong and partly support by Project No. 51707171 under National Natural Science Foundation, China.

References

[1] Z. Q. Zhu and D. Howe, "Electrical Machines and Drives for Electric, Hybrid, and Fuel Cell Vehicles," in *Proceedings of the IEEE*, vol. 95, no. 4, pp. 746-765, April 2007.

[2] K. T. Chau, C. C. Chan and C. Liu, "Overview of Permanent-Magnet Brushless Drives for Electric and Hybrid Electric Vehicles," in *IEEE Transactions on Industrial Electronics*, vol. 55, no. 6, pp. 2246-2257, June 2008.

[3] X. Zhao and S. Niu, "A New Slot-PM Vernier Reluctance Machine with Enhanced Zero-Sequence Current Excitation for Electric Vehicle Propulsion," in *IEEE Transactions on Industrial Electronics*, vol. 67, no. 5, pp. 3528-3539, May 2020.

[4] G. Pellegrino, A. Vagati, P. Guglielmi and B. Boazzo, "Performance Comparison Between Surface-Mounted and Interior PM Motor Drives for Electric Vehicle Application," in *IEEE Transactions on Industrial Electronics*, vol. 59, no. 2, pp. 803-811, Feb 2012.

[5] B. Sarlioglu and C. T. Morris, "More Electric Aircraft: Review, Challenges, and Opportunities for Commercial Transport Aircraft," in *IEEE Transactions on Transportation Electrification*, vol. 1, no. 1, pp. 54-64, June 2015.

[6] V. Madonna, P. Giangrande and M. Galea, "Electrical Power Generation in Aircraft: Review, Challenges, and Opportunities," in *IEEE Transactions on Transportation Electrification*, vol. 4, no. 3, pp. 646-659, Sept 2018.

[7] X. Zhao and S. Niu, "A New Slot-PM Vernier Reluctance Machine with Enhanced Zero-Sequence Current Excitation for Electric Vehicle Propulsion," in *IEEE Transactions on Industrial Electronics*, vol. 67, no. 5, pp. 3528-3539, May 2020.

[8] X. Zhao, S. Niu, X. Zhang and W. Fu, "Flux-Modulated Relieving-DC-Saturation Hybrid Reluctance Machine with Synthetic Slot-PM Excitation for Electric Vehicle In-Wheel Propulsion," in *IEEE Transactions on Industrial Electronics*, vol. 68, no. 7, pp. 6075-6086, July 2021.

[9] J. Ye, B. Bilgin and A. Emadi, "An Extended-Speed Low-Ripple Torque Control of Switched Reluctance Motor Drives," in *IEEE Transactions on Power Electronics*, vol. 30, no. 3, pp. 1457-1470, March 2015.

[10] S. Mir, M. E. Elbuluk and I. Husain, "Torque-ripple minimization in switched reluctance motors using adaptive fuzzy control," in *IEEE Transactions on Industry Applications,* vol. 35, no. 2, pp. 461-468, Mar. 1999.

[11] P. Andrada, B. Blanqué, E. Martínez, M. Torrent, "A novel type of hybrid reluctance motor drive", in *IEEE Transactions on Industrial Electronics*, vol. 61, no. 8, pp. 4337-4345, Aug. 2014.

[12] S. Ullah, S. P. McDonald, R. Martin, M. Benarous and G. J. Atkinson, "A Permanent Magnet Assist, Segmented Rotor, Switched Reluctance Drive for Fault Tolerant Aerospace Applications," in *IEEE Transactions on Industry Applications*, vol. 55, no. 1, pp. 298-305, Jan.-Feb. 2019.

[13] Z. Bian, Z. Zhang and L. Yu, "Synchronous Commutation Control of Doubly Salient Motor Drive with Adaptive Angle Optimization," in *IEEE Transactions on Power Electronics*, vol. 35, no. 6, pp. 6070-6081, June 2020.

[14] Z. Chen, and Y. Yan "A doubly salient starter/generator with two-section twisted-rotor structure for potential future aerospace application," in *IEEE Transactions on Industrial Electronics*, vol. 59, no. 9, pp. 3588-3595, Sept. 2012.

[15] Y. Wang, Z. Zhang, and Y. Yan, "Torque density improvement of doubly salient electromagnetic machine with asymmetric current control," in *IEEE Transactions on Industrial Electronics*, vol. 63, no. 12, pp. 7434-7443, Dec. 2016.

[16] X. Liu and Z. Q. Zhu, "Stator/Rotor Pole Combinations and Winding Configurations of Variable Flux Reluctance Machines," in *IEEE Transactions on Industry Applications*, vol. 50, no. 6, pp. 3675-3684, Nov.-Dec. 2014.

[17] Z. Q. Zhu, B. Lee and X. Liu, "Integrated field and armature current control strategy for variable flux reluctance machine using open winding," in *IEEE Transactions on Industry Applications*, vol. 52, no. 2, pp. 1519-1529, Mar. 2016.

[18] X. Zhao, S. Niu, X. Zhang and W. Fu, "Design of a New Relieving-DC-Saturation Hybrid Reluctance Machine for Fault-Tolerant In-Wheel Direct Drive," in *IEEE Transactions on Industrial Electronics*, vol. 67, no. 11, pp. 9571-9581, Nov. 2020.

[19] A. Fasolo, L. Alberti and N. Bianchi, "Performance Comparison Between Switching-Flux and IPM Machines with Rare-Earth and Ferrite PMs," in *IEEE Transactions on Industry Applications*, vol. 50, no. 6, pp. 3708-3716, Nov.-Dec. 2014.

[20] X. Zhao and S. Niu, "Design and Optimization of a New Magnetic-Geared Pole-Changing Hybrid Excitation Machine," in *IEEE Transactions on Industrial Electronics*, vol. 64, no. 12, pp. 9943-9952, Dec. 2017.

[21] Z. S. Du and T. A. Lipo, "Design of an Improved Dual-Stator Ferrite Magnet Vernier Machine to Replace an Industrial Rare-Earth IPM Machine," in *IEEE Transactions on Energy Conversion*, vol. 34, no. 4, pp. 2062-2069, Dec. 2019.

[22] X. Zhao, S. Niu and W. Fu, "Sensitivity Analysis and Design Optimization of a New Hybrid-Excited Dual-PM Generator with Relieving-DC-Saturation Structure for Stand-Alone Wind Power Generation," in *IEEE Transactions on Magnetics*, vol. 56, no. 1, pp. 1-5, Jan. 2020.

[23] I. Petrov, M. Niemelä, P. Ponomarev and J. Pyrhönen, "Rotor Surface Ferrite Permanent Magnets in Electrical Machines: Advantages and Limitations," in *IEEE Transactions on Industrial Electronics*, vol. 64, no. 7, pp. 5314-5322, July 2017.